Published in final edited form as:
J Med Chem. 2013 November 14; 56(21): 8270–8279. doi:10.1021/jm400899c.

Discovery and Optimization of Piperidyl-1,2,3-Triazole Ureas as Potent, Selective, and *In Vivo*-Active Inhibitors of Alpha/Beta-Hydrolase Domain Containing 6 (ABHD6)

Ku-Lung Hsu[1,2,*,†], **Katsunori Tsuboi**[1,2,†], **Jae Won Chang**[1,2], **Landon R. Whitby**[1,2], **Anna E. Speers**[1,2], **Holly Pugh**[2], and **Benjamin F. Cravatt**[1,2,*]

[1]The Skaggs Institute for Chemical Biology, La Jolla, California, USA. Department of Chemical Physiology, The Scripps Research Institute, La Jolla, California, USA

[2]The Scripps Research Institute, La Jolla, California, USA. Department of Chemical Physiology, The Scripps Research Institute, La Jolla, California, USA

Abstract

Alpha/beta-hydrolase domain containing 6 (ABHD6) is a transmembrane serine hydrolase that hydrolyzes the endogenous cannabinoid 2-arachidonoylglycerol (2-AG) to regulate certain forms of cannabinoid receptor-dependent signaling in the nervous system. The full spectrum of ABHD6 metabolic activities and functions is currently unknown and would benefit from selective, *in vivo*-active inhibitors. Here, we report the development and characterization of an advanced series of irreversible (2-substituted)-piperidyl-1,2,3-triazole urea inhibitors of ABHD6, including compounds KT182 and KT203, which show exceptional potency and selectivity in cells (< 5 nM) and, at equivalent doses in mice (1 mg kg^{-1}), served as systemic and peripherally-restricted ABHD6 inhibitors, respectively. We also describe an orally-bioavailable ABHD6 inhibitor KT185 that displays excellent selectivity against other brain and liver serine hydrolases *in vivo*. We thus describe several chemical probes for biological studies of ABHD6, including brain-penetrant and peripherally-restricted inhibitors that should prove of value for interrogating ABHD6 function in animal models.

Introduction

The alpha/beta-hydrolase domain containing 6 (ABHD6) gene encodes a ~35 kDa protein containing an N-terminal transmembrane region followed by a catalytic domain that includes the canonical GXSXG active-site motif of serine hydrolases (SHs). ABHD6 is a

[*]Corresponding Author: Authors to whom correspondence should be addressed: kenhsu@scripps.edu (K.L.H.), Department of Chemical Physiology, The Skaggs Institute for Chemical Biology, The Scripps Research Institute, SR107, 10550 North Torrey Pines Road, La Jolla, CA 92037, Phone: 858 784-8636, cravatt@scripps.edu (B.F.C.); Department of Chemical Physiology, The Skaggs Institute for Chemical Biology, The Scripps Research Institute, SR107, 10550 North Torrey Pines Road, La Jolla, CA 92037, Phone: 858 784-8633.
[†]**Author Contributions**: These authors contributed equally to this work

Supporting Information: Supplemental methods, synthetic procedures and characterization of 1,2,3-triazole ureas, ^{1}H NMR spectra, HRMS data, and supplemental figures. This material is available free of charge via the Internet at http://pubs.acs.org.

Notes: The authors declare the following competing financial interest(s): Dr. Cravatt is a founder and adviser to Abide Therapeutics a biotechnology company interested in developing serine hydrolase inhibitors as drugs to treat human disease.

unique and highly conserved enzyme in mammals (94% sequence identity between human and mouse orthologues, ~25% identity to the nearest homologous enzyme - SERHL) and is expressed prominently in brain, liver, kidney, and brown adipose tissue based on global gene expression analysis (http://biogps.gnf.org/) and activity-based protein profiling (ABPP).[1] As a member of the SH class, ABHD6 is predicted to hydrolyze ester, amide, or thioester bonds in substrates that could include small-molecules, lipids, or peptides, although the full range of substrates regulated by this enzyme *in vivo* is currently unknown.[2]

Chemical proteomic studies led to the discovery that ABHD6 can hydrolyze the endogenous cannabinoid (endocannabinoid), 2-arachidonoylglycerol (2-AG) *in vitro*[3] and, in support of this metabolic function, inactivation of ABHD6 by first-generation carbamate inhibitors[4] alters cannabinoid receptor-dependent synaptic signaling in mouse cortical slices.[3, 5] Recent studies have also shown that ABHD6 carbamate inhibitors produce anti-inflammatory and neuroprotective effects in a mouse model of traumatic brain injury.[6] Whether the neuroprotective effects of these inhibitors are mediated by elevations in 2-AG or a novel ABHD6-regulated metabolite, however, remains unknown. While first-generation carbamate compounds exhibit good inhibitory activity against ABHD6 *in vitro* (IC_{50} value of ~70-85 nM),[4, 7] next-generation inhibitors with improved potency, selectivity, and *in vivo* activity would facilitate the functional analysis of ABHD6 in mammalian biology and disease.

In recent studies focused on developing inhibitors of the endocannabinoid biosynthetic enzyme DAGLβ,[8, 9] we identified a (2-phenyl)-piperidyl-1,2,3-triazole urea [(2-phenyl)-Pip-1,2,3-TU] inhibitor of ABHD6 termed compound **1** (KT195),[8] which is predicted to irreversibly inhibit ABHD6 by carbamoylation of the enzyme's serine nucleophile.[8] Here, we describe the further optimization of (2-substituted)-Pip-1,2,3-TU inhibitors of ABHD6[10] and show that the addition of polar substituents onto the biphenyl-triazole group can fine-tune the potency, selectivity, and *in vivo* activity of compounds, resulting in development of the highly potent (IC_{50} values ~ 1 nM) and selective ABHD6 inhibitors, **9** (KT182) and **20** (KT203), that show systemic and peripherally restricted activity, respectively, as well as the first orally-active ABHD6-selective inhibitor, **11** (KT185). These findings highlight the versatility of 1,2,3-TUs as inhibitors of ABHD6, which combine simplified synthetic routes with the ability to achieve excellent potency and selectivity and controlled access to the central nervous system (CNS) for developing peripherally-restricted chemical probes.

Results

A clickable probe to evaluate the proteome-wide selectivity of compound 1

Previous studies using both gel- and MS-based competitive ABPP[8] showed that compound **1** (Table 1) exhibits excellent potency (*in vitro* IC_{50} of ~10 nM) and selectivity for ABHD6 across the SH family, but did not address potential for cross-reactivity with other proteins in the proteome. To assess the broader, proteome-wide selectivity of compound **1**, we synthesized an alkynylated analog **2** (Figure 1A), such that the alkyne group would serve as a latent affinity handle suitable for conjugation to reporter tags by copper-catalyzed azide alkyne cycloaddition[11] (CuAAC or click chemistry). We confirmed that compound **2** maintained good inhibitory activity against ABHD6 as measured by gel-based competitive ABPP in mouse neuroblastoma Neuro2A cell and mouse brain proteomes (Figure 1B, C).

Next, we treated Neuro2A cells with varying concentrations of compound **2** for 1 hr. Cells were then lysed and the membrane proteomes conjugated by click chemistry with an azide-Rh tag,[12] separated by SDS-PAGE, and probe-labeled proteins visualized by in-gel fluorescence scanning (Figure 1D). This analysis revealed a single major protein target of ~ 35 kDa, matching the molecular mass of ABHD6, that could be detected at concentrations of compound **2** as low as 10 nM (Figure 1D). At higher concentrations (80-600 nM) of **2**, some limited cross-reactivity was observed, mainly with a 60 kDa protein that likely represents fatty acid amide hydrolase (FAAH), a known, lower affinity off-target of compound **1** (Table 1). We confirmed that compound **2** is cross-reactive with FAAH in the mouse brain proteome at concentrations of 0.4 – 10 μM as judged by competitive ABPP (Figure 1C). Considering that compound **1** completely inactivates ABHD6 (with negligible cross-reactivity with FAAH) at concentrations of 25 nM in living cells,[8] our data argue that **1** exhibits excellent proteome-wide selectivity at concentrations required to inhibit ABHD6 *in situ*. When combined with complementary studies of clickable probes for 2-substituted Pip-1,2,3-TU inhibitors of DAGL enzymes, which also showed good proteome-wide selectivity at concentrations of 80 nM or below,[9] our results suggest further that the (2-substituted)-Pip-1,2,3-TU chemotype is generally suitable for creating selective SH inhibitors, especially if the *in situ* potencies of these agents can be optimized to the low (< 100 nM) range.

Optimization of (2-substituted)-Pip-1,2,3-TUs as ABHD6 inhibitors

In our previous studies, we used compound **1** primarily as a control probe for evaluating the activity of structurally related DAGLβ inhibitors.[8] Consequently, the structure-activity relationship for (2-substituted)-Pip-1,2,3-TU-ABHD6 interactions was not explored. Here, we set out to address this question by testing the activity of structurally diverse analogues of **1** to identify ABHD6 inhibitors with improved *in vitro* potency and *in vivo* activity. We first compared the activity of several compounds that contained polar groups on the biphenyl triazole group (Table 1 and Figure 2). As reported previously, 2-benzyl compounds, such as **3** (KT172),[8] **4** (KT123),[9] and **5** (KT125),[9] exhibited high-potency for ABHD6, but also cross-reacted with DAGLβ (Figure 2A, B and Table 1). Inclusion of polar groups at the 3 or 4 positions of the distal phenyl ring on the biphenyl triazole leaving group improved selectivity against DAGLβ (Figure 2A, B and Table 1), as well as eliminating monoacylglycerol lipase (MGLL) as an off-target at higher concentrations (Figure 2C and Table 1). Substitution of the 2-benzyl for a 2-phenyl group (compounds **1** and **6**) nearly eliminated DAGLβ cross-reactivity with minimal loss in potency towards ABHD6 (Figure 2A, B and Table 1). However, this alteration also introduced FAAH as an additional off-target at higher inhibitor concentrations (10 μM).

We next aimed to improve the potency and selectivity of (2-phenyl)-Pip-1,2,3-TUs by further exploring various polar substitutions (hydroxymethyl, **8**-**10**; secondary amide, **11** and **12**; or primary amide, compound **13**) on the biphenyl triazole group (Scheme 1). In brief, the 4-bromo-triazole ring was synthesized using the copper-catalyzed azide-alkyne cycloaddition reaction[14] and coupled to 2-phenyl piperidine to generate compound **7** as previously described.[8, 15] Compounds **8**-**13** were synthesized using **7** as the key intermediate for subsequent Suzuki coupling reactions (Scheme 1). We compared the *in vitro* potency of

compounds against endogenous ABHD6 in mouse brain or Neuro2A membrane proteomes by gel-based competitive ABPP utilizing the broad-spectrum and tailored SH activity-based probes, fluorophosphonaterhodamine (FP-Rh) and HT-01, respectively, as described previously.[8]

All of the synthesized derivatives (**8**-**13**), when tested at 1 μM, selectively inhibited ABHD6 among mouse brain SHs, but showed variable levels of off-target activity at 10 μM (Figure 3A, B and Table 2). We consistently observed increased inhibitory activity against ABHD6 for compounds with modifications at the 2- (**8**) and 3-positions (**9** and **11**) compared with their respective 4-substituted derivatives (**10, 12**, and **13**). From this series of compounds, we selected compounds **9** and **11** as suitable for further investigation. Compound **9** was chosen based on its improved selectivity over **8** (i.e., attenuated activity against LYPLA1 and LYPLA2; Figure 3B) and its smaller molecular weight in comparison with **12** (MW < 500). Compound **11** was selected based on its enhanced selectivity against FAAH and other SHs when tested at high concentrations in the mouse brain (10 μM, Figure 3B).

We also synthesized a series of carboxylic acid derivatives by coupling amines with a 4-bromo-triazole group to form intermediates **7**, **14**, and **15**, which were then converted into corresponding 3-benzylcarboxyphenyl derivatives by Suzuki coupling reactions (**17** – **19**) (Scheme 2). Subsequent treatment of benzylcarboxyphenyl intermediates with 10% Pd-C under hydrogen atmosphere generated the carboxylic acid derivatives (**20** – **22**). We found that substitution of a hydroxymethyl for a carboxylate group at the 3-position of the distal phenyl ring of the triazole-biphenyl group preserved potency for ABHD6 (compare profiles of **9** and **21** in Figure 2A and Table 2), but increased off-target interactions in the mouse brain proteome, where **21 (**at 1 μM) also inhibited APEH, LYPLA1, and LYPLA2 (Figure 3B and Table 2). Substitution of the 2-phenyl (**21**) for a 2-benzyl (**20**) but not a 2-phenethyl (**22**) group improved both potency and overall selectivity with no observable SH off-targets at 1 μM other than a modest 50% inhibition of DAGLβ (Figure 3A, B and Table 2). Given its potency, selectivity, and increased polarity, compound **20** was designated as a third ABHD6 inhibitor worthy of more detailed analysis.

(2-substituted)-Pip-1,2,3-TUs are potent and selective ABHD6 inhibitors *in situ*

We next measured *in vitro* potencies for compounds **9**, **11**, and **20** and found that all three compounds potently inhibited ABHD6 as measured by gel-based competitive ABPP (IC_{50} values between 0.8 - 1.7 nM, Figure 4A, B) and 2-AG hydrolysis assays (IC_{50} values between 3.9 – 15.1 nM, Figure 4C). *In situ* potencies were then measured by treating Neuro2A cells with varying concentrations of compounds for 4 hr, after which cells were lysed and proteomes subjected to gel-based ABPP as previously described.[8] We found that all three compounds inhibited ABHD6 *in situ* with IC_{50} values in the subnanomolar range (0.2 - 0.3 nM, Figure 4D, E). For comparison, compounds **9**, **11**, and **20** were ~10-fold and ~5-fold more potent *in vitro* and *in situ*, respectively, compared to compound **1**.[8]

To more comprehensively profile the selectivity of compounds **9**, **11**, and **20** in cells, we utilized a quantitative mass-spectrometry (MS)-based proteomic method termed ABPP-SILAC.[8, 15, 16] In brief, Neuro2A cells cultured in “light” ($^{12}C_6{}^{14}N_2$-lysine and $^{12}C_6{}^{14}N_2$-

arginine) or "heavy" medium ($^{13}C_6{}^{15}N_2$-lysine and $^{13}C_6{}^{15}N_2$-arginine) were treated with DMSO or inhibitors (3 nM, 4 hr), respectively, lysed, proteomes separated into soluble and membrane fractions, and SHs enriched with FP-biotin (10 μM, 2 hr). Heavy (inhibitor-treated) and light (DMSO-treated) fractions were then mixed 1:1, enriched with avidin, digested on-bead with trypsin, and analyzed by liquid chromatography-tandem mass spectrometry (LC-MS/MS) using an LTQ-Orbitrap instrument. Light and heavy signals were quantified from parent ion peaks (MS1) and the corresponding proteins identified from product ion profiles (MS2) using the SEQUEST search algorithm. The depicted bar graphs represent the average ratios of quantified heavy/light tryptic peptides for >50 SHs identified in the Neuro2A proteome (Figure 5). We found that both compound **9** and **20** blocked > 90% of ABHD6 activity, while **11** blocked > 80% of ABHD6 activity in Neuro2A cells, and, importantly, none of the compounds showed substantial cross-reactivity (< 50%) against the ~50 other SHs detected in this cell line (Figure 5). Collectively, these results show that compounds **9**, **11**, and **20** potently and selectively inhibit ABHD6 in living cells.

Compounds 9 and 20 are potent and selective ABHD6 inhibitors *in vivo*

Mice were treated intraperitoneally (i.p., 18:1:1 solution of saline/ethanol/PEG40 (ethoxylated castor oil), 10 μL g^{-1}) with compound **9** or **20** at various doses (0.1 – 1 mg kg^{-1}) for 4 hr, sacrificed, and brain and liver tissue collected for analysis by gel-based competitive ABPP using HT-01 and FP-Rh probes. Both compound **9** and **20** produced near-complete blockade of ABHD6 in the liver at the highest dose tested (1 mg kg^{-1}, HT-01 gels, Figure 6A). At lower doses, the compounds maintained ~80% inhibition of ABHD6 in the liver with **20** showing slightly enhanced potency compared to **9** at the lowest dose tested (0.1 mg kg^{-1}, Figure 6A). Notably, both compound **9** and **20** showed impressive selectivity in the mouse liver even at higher doses (1 mg kg^{-1}), exhibiting little cross-reactivity against the numerous carboxylesterase enzymes (CESs) that are common off-targets of mechanism-based SH inhibitors in rodents.[1, 8, 17] Compound **9** also completely inactivated ABHD6 in the mouse brain at 1 mg kg^{-1} (Figure 6B). In contrast, compound **20** showed negligible inhibition of brain ABHD6 at all doses tested (Figure 6B). Both compounds showed good selectivity against other brain and liver SHs as judged by gel-based ABPP (FP-Rh gels, Figure 6), which revealed only a single off-target, carboxylesterase-1 (CES1), a plasma esterase that exhibits broad reactivity with various classes of SH inhibitors[1] and was inhibited in our study by **9**, but not **20**. These data confirm that compounds **9** and **20** are potent and selective ABHD6 inhibitors *in vivo*, showing systemic- and peripherally-restricted activity, respectively. Considering that compounds **9** and **20** displayed similar potencies against liver ABHD6 *in vivo*, we believe that the reduced activity of **20** against brain ABHD6 likely reflects diminished CNS penetrance possibly due to it unique carboxylic acid substituent.

Compound 11 is an orally-bioavailable and selective ABHD6 inhibitor *in vivo*

Our *in vivo* studies with **11** revealed that this compound was systemically active, but exhibited reduced potency in mice compared to **9**, requiring ~40 mg/kg (i.p.) to completely block ABHD6 in the brain (Figure 7A). In the liver we observed near-complete blockade of ABHD6 at doses as low as 5-10 mg/kg (i.p., Supplementary Figure 2) suggesting that this

compound shows reduced central activity akin to **20**. However, at all doses tested, compound **11** maintained excellent selectivity for ABHD6 over other brain SHs, including FAAH (Figure 7B), against which this compound showed superior selectivity compared with compounds **9** and **20** at high concentrations *in vitro* (Figure 3B). We also found that compound **11** was orally active in mice (p.o., PEG300 vehicle, 4 μL g^{-1}, 4 hr), producing complete blockade of brain ABHD6 at 40 mg/kg as measured by gel-based competitive ABPP using HT-01 and FP-Rh (Figure 7B) with the only detectable off-target being CES1. These results contrasted with the activity of compounds **9** and **20**, which showed cross-reactivity with FAAH in the brains of mice treated by oral gavage with doses as low as 10 mg kg^{-1} (Supplementary Figure 1). We also observe near-complete blockade of ABHD6 at doses of 10 – 40 mg/kg and minimal cross-reactivity with CESs (other than CES1) in liver of compound **11**-treated mice (Supplementary Figure 2). These data confirm that compound **11** is an orally-bioavailable and selective ABHD6 inhibitor *in vivo*, showing minimal cross-reactivity with other SHs in the mouse brain and liver across a broad dose-range.

Conclusion

Despite emerging roles for ABHD6 in endocannabinoid metabolism, neural signaling, and neurodegeneration,[3, 5, 6] the full spectrum of endogenous substrates regulated by this enzyme remains poorly characterized due in part to the lack of optimized inhibitors for functional studies *in vivo*. Here, we have addressed this problem by developing several new chemical probes including brain-penetrant and peripherally-restricted inhibitors of ABHD6.

In previous studies, we described compound **1** as a lead (2-phenyl)-Pip-1,2,3-TU inhibitor of ABHD6 and its use as a control probe in our characterization of structurally-related DAGLβ inhibitors.[8] Here, we aimed to improve the *in vitro* and *in vivo* activity of 2-substituted Pip-1,2,3-TU inhibitors by performing a more comprehensive exploration of the structure-activity relationship underlying their interactions with ABHD6. We discovered that the potency and selectivity of lead compounds could be affected by the addition of polar substituents to the triazole group. This modification, combined with replacing the 2-benzyl with a 2-phenyl moiety on the piperidine group eliminated most of the off-targets for (2-substituted)-Pip-1,2,3-TUs, including DAGLβ. Our ABPP-guided medicinal chemistry efforts culminated in the development of the optimized ABHD6 inhibitors, **9**, **11**, and **20** that all showed improved potency (~10-fold enhancement, Figure 4A and C) and selectivity *in vitro* compared with compound **1**.[8]

We proceeded to demonstrate that compounds **9**, **11**, and **20** were potent and selective ABHD6 inhibitors in cells (IC_{50} values of 0.2 – 0.3 nM, Figure 4C and D), displaying negligible cross-reactivity against the other 50+ SHs detected in Neuro2A cells as evaluated by ABPP-SILAC[8, 15, 16] (Figure 5). While compounds **9** and **20** shared similar properties with respect to potency and selectivity in cells, they displayed different activity profiles *in vivo*. Treatment of mice with compound **9** inactivated ABHD6 in both the brain and liver (Figure 6). In contrast, compound **20** produced negligible inhibition of ABHD6 in the brain, but near-complete blockade of ABHD6 in the liver (Figure 6). Both compounds displayed good selectivity *in vivo* as judged by gel-based competitive ABPP with the FP-Rh and HT-01 probes. Our studies thus indicate that compounds **9** and **20** can be used as paired

probes to distinguish the effects of peripheral and central inactivation of ABHD6 *in vivo*. We also found that compound **11** selectively inactivated ABHD6 in mice when administered intraperitoneally or by oral gavage. Taken together, our data demonstrates that (2-substituted)-piperidyl-1,2,3-triazole ureas can be fine-tuned to create selective ABHD6 inhibitors with good *in vivo* activity. These inhibitors should serve as valuable chemical probes for characterizing ABHD6 function in cell and animal models.

Experimental Section

Materials Used for Biological Experiments

Pharmacological studies were conducted in C57Bl/6 mice. The fluorophosphonate and HT-01 activity-based probes were synthesized as previously described.[8, 18, 19] HEK293T and Neuro2A cells were purchased from ATCC. All lipids used in substrate assays were purchased from Cayman Chemicals or Avanti Lipids.

Synthetic Methods

Commercially-available chemicals and reagents were purchased from the following vendors: Sigma-Aldrich, Acros, Fisher, Fluka, Maybridge, Combi-Blocks, BioBlocks, and Matrix Scientific and used without further purification unless noted otherwise. Dry solvents were obtained by passing commercially available pre-dried, oxygen-free formulations through activated alumina columns. Reactions were performed under a nitrogen atmosphere using oven-baked glassware unless otherwise noted. Flash chromatography was performed using 230-400 mesh silica gel. Reactions were monitored by analytical thin-layer chromatography (TLC) on precoated, glass backed silica gel 60 F_{254} plates. Reactions were purified either by pTLC, also on silica gel 60 F_{254} plates or by flash chromatography on 40-60 MYM mesh silica gel as specified. ^{1}H-NMR and spectra were recorded in $CDCl_3$ on a Varian Mercury-300 spectrometer, a Varian Inova-400 or a Bruker DRX-600 spectrometer, and were referenced to trimethylsilane (TMS). Chemical shifts were reported in ppm relative to TMS and *J* values were reported in Hz. High resolution mass spectrometry (HRMS) experiments were performed at The Scripps Research Institute Mass Spectrometry Core on an Agilent mass spectrometer using electrospray ionization-time of flight (ESI-TOF). All final compounds were determined to be >95% pure by HPLC analysis (Agilent 1100 LC/MS).

(4-(3′-(Hydroxymethyl)-[1,1′-biphenyl]-4-yl)-1H-1,2,3-triazol-1-yl)(2-phenylpiperidin-1-yl)methanone (9)—A solution of KT179[8] (**7**) (0.70 g, 1.7 mmol) in dioxane (30 mL) and H_2O (3 mL) was treated with 3-hydroxymethylphenyl boronic acid (0.39 g, 2.6 mmol, 1.5 equiv), K_2CO_3 (0.70 g, 5.1 mmol, 3.0 equiv) and $PdCl_2$(dppf) (62 mg, 0.085 mmol, 0.2 equiv), and the reaction mixture was stirred for 2 hr at 80 °C under N_2. The mixture was poured into H_2O and extracted with ethyl acetate. The organic layer was washed with H_2O and brine, dried over Na_2SO_4 and concentrated under reduced pressure. Chromatography (150 g, ethyl acetate:hexane=1:1) afforded **9** (0.55 g, 1.26 mmol, 74%). The final compound was purified as the racemate, which was suitable for biological studies.[9]

^{1}H NMR ($CDCl_3$, 300 MHz) δ 8.44 (s, 1H), 7.96 (d, 2H, *J* = 8.3 Hz), 7.70 (d, 2H, *J* = 8.3 Hz), 7.65 (s, 1H), 7.58 (m, 1H), 7.48-7.25 (m, 7H), 5.93 (br, 1H), 4.78 (br, 2H), 4.38 (brd, 1H, *J* = 13.5 Hz), 3.19 (m, 1H), 2.53 (brd, 1H, *J* = 14.1 Hz), 2.16 (m, 1H), 1.90-1.65 (m, 4H). ^{13}C NMR ($CDCl_3$, 151 MHz) δ 176.96, 149.78, 146.88, 141.86, 141.52, 141.10, 138.20, 129.45, 129.31, 128.95, 128.01, 127.53, 126.92, 126.65, 126.48, 125.94, 121.34, 65.68, 28.13, 26.19, 19.66. HRMS calculated for $C_{27}H_{27}N_4O_2$ $[M+H]^+$ 439.2128, found 439.2116.

(2-Phenylpiperidin-1-yl)(4-(3′-(piperidine-1-carbonyl)-[1,1′-biphenyl]-4-yl)-1H-1,2,3-triazol-1-yl)methanone (11)—A solution of **7** (10 mg, 0.024 mmol) in dioxane (1 mL) and H_2O (0.1 mL) was treated with (3-(piperidine-1-carbonyl)phenyl)boronic acid (8 mg, 0.036 mmol, 1.5 equiv), K_2CO_3 (10 mg, 0.072 mmol, 3.0 equiv) and $PdCl_2$(dppf) (4 mg, 0.0049 mmol, 0.2 equiv), and the reaction mixture was stirred for 2 hr at 80 °C under N_2. The mixture was poured into H_2O and extracted with ethyl acetate. The organic layer was washed with H_2O and brine, dried over Na_2SO_4 and concentrated under reduced pressure. The crude oil was purified by pTLC (ethyl acetate:hexane = 1:1) to give **11** (4 mg, 0.008 mmol, 32%).

^{1}H NMR ($CDCl_3$, 300 MHz) δ 8.45 (s, 1H), 7.96 (d, 2H, *J* = 8.3 Hz), 7.72-7.64 (m, 4H), 7.53-7.25 (m, 7H), 5.93 (br, 1H), 4.38 (brd, 1H, *J* = 12.7 Hz), 3.74 (br, 2H), 3.40 (br, 2H), 3.19 (m, 1H), 2.54 (brd, 1H, *J* = 14.3 Hz), 2.16 (m, 1H), 1.90-1.50 (m, 10H). ^{13}C NMR ($CDCl_3$, 151 MHz) δ 176.97, 170.44, 149.76, 146.78, 141.04, 140.95, 138.19, 137.52, 129.24, 128.24, 128.01, 127.53, 126.92, 126.72, 126.18, 125.72, 121.41, 49.20, 43.50, 30.04, 28.18, 26.98, 26.18, 25.97, 24.94, 19.66. HRMS calculated for $C_{32}H_{34}N_5O_2$ $[M+H]^+$ 520.2707, found 520.2708.

Benzyl 4′-(1-(2-benzylpiperidine-1-carbonyl)-1H-1,2,3-triazol-4-yl)-[1,1′-biphenyl]-3-carboxylate (17)—A solution of **14** (1.2 g, 2.9 mmol) in dioxane (40 mL) and H_2O (4 mL) was treated with 3-carboxybenzylphenyl bronic acid (1.1 g, 4.4 mmol, 1.5 equiv), K_2CO_3 (1.2 g, 8.7 mmol, 3.0 equiv) and $PdCl_2$(dppf) (0.11 g, 0.15 mmol, 0.05 equiv), and the reaction mixture was stirred for 2 hr at 80 °C under N_2. The mixture was poured into H_2O and extracted with ethyl acetate. The organic layer was washed with H_2O and brine, dried over Na_2SO_4 and concentrated under reduced pressure. Chromatography (150 g, ethyl acetate:hexane=1:3) afforded **17** (1.6 g, quantitative).

^{1}H NMR ($CDCl_3$, 300 MHz) δ 8.36 (s, 1H), 8.08 (d, 1H, *J* = 7.5 Hz), 7.89 (br, 2H), 7.84 (d, 1H, *J* = 7.3 Hz), 7.71 (d, 2H, *J* = 8.4 Hz), 7.56-7.33 (m, 6H), 7.30-6.90 (m, 5H), 5.42 (s, 2H), 4.86 (br, 1H), 4.37 (d, 1H, *J* = 13.3 Hz), 3.48-2.69 (m, 3H), 2.05-1.65 (m, 6H). HRMS calculated for $C_{35}H_{33}N_4O_3$ $[M+H]^+$ 557.2547, found 557.2552.

4′-(1-(2-Benzylpiperidine-1-carbonyl)-1H-1,2,3-triazol-4-yl)-[1,1′-biphenyl]-3-carboxylic acid (20)—A solution of **17** (1.6 g, 2.9 mmol) in THF (30 mL) was treated with 10% Pd-C (0.30 g) and the mixture was stirred overnight at room temperature under N_2. The mixture was passed through Celite and the filtrate was concentrated under reduced pressure. Crystallization from ethyl acetate and hexane afforded **20** (KT203) (1.2 g, 2.6 mmol, 89%).

^{1}H NMR ($CDCl_3$, 300 MHz) δ 8.41 (s, 1H), 8.12 (d, 1H, *J* = 7.8 Hz), 7.95-7.84 (m, 3H), 7.73 (d, 2H, *J* = 8.3 Hz), 7.59 (t, 1H, *J* = 7.8 Hz), 7.50-6.95 (m, 5H), 5.30 (br, 1H), 4.37 (brd, 1H, *J* = 13.8 Hz), 3.48-2.60 (m, 3H), 2.05-1.65 (m, 6H). ^{13}C NMR ($CDCl_3$, 151 MHz) δ 176.95, 171.95, 149.63, 146.22, 141.22, 140.27, 138.29, 132.54, 130.30, 129.54, 129.51, 129.45, 129.07, 129.03, 127.99, 126.94, 126.63, 121.03, 57.75, 41.27, 36.98, 29.23, 25.64, 19.21. HRMS calculated for $C_{28}H_{27}N_4O_3$ $[M+H]^+$ 467.2078, found 467.2077.

2-AG substrate hydrolysis assay

The activity of ABHD6 was determined using recombinant mouse ABHD6 protein overexpressed in HEK293T cells using a previously described 2-AG LC-MS hydrolysis assay with some minor modifications.[3] HEK293T-ABHD6 membrane lysates were diluted to 0.2 mg/mL in assay buffer (PBS + 0.05% Triton X-100, 50 μL reaction volume). Lysates were treated with DMSO or compound for 30 min at 37 °C. The substrate was prepared by sonicating 2-arachidonoylglycerol (2-AG) in PBS + 0.05% Triton X-100. The substrate was added to the sample reaction (50 μL, 100 μM final concentration of 2-AG) and incubated for 30 min at 37 °C. The reaction was quenched by adding 300 μL of 2:1 v/v $CHCl_3$:MeOH, doped with 1 nmol of pentadecanoic acid standard, vortexed and then centrifuged (1,400 × *g*, 3 min) to separate the phases. The organic phase was subjected to LC-MS analysis and arachidonic acid release was quantified as previously described.[3]

Preparation of cell line proteomes

HEK293T and Neuro2A cells were grown in DMEM supplemented with 10% fetal bovine serum at 37 °C with 5% CO_2. For *in vitro* experiments, cells were grown to 80-90% confluency, washed twice with cold PBS (pH 7.5) and scraped. Cell pellets were then isolated by centrifugation at 1,400 × *g*, for 3 min at 4 °C. The pellets were resuspended in 500 μL of cold PBS (pH 7.5), sonicated, and centrifuged (100,000 × *g*, 45 min) to generate soluble and membrane fractions. Mouse DAGLβ was transiently overexpressed in HEK293T cells as previously described.[8] Total protein concentration of membrane and soluble fractions was determined using a protein assay kit (Bio-Rad). Samples were stored at -80 °C until use.

Preparation of mouse tissue proteomes

Brains and livers from C57Bl/6 mice were Dounce-homogenized in PBS, pH 7.5, followed by a low-speed spin (1,400 × *g*, 5 min) to remove debris. The supernatant was then centrifuged at 100,000 × *g*, for 45 min to generate the cytosolic fraction in the supernatant and the membrane fraction as a pellet. The pellet was washed and resuspended in PBS buffer by sonication. The total protein concentration in each fraction was determined using a protein assay kit (Bio-Rad). Samples were stored at -80 °C until further use.

Gel-based competitive ABPP

Gel-based competitive ABPP experiments were performed as previously described.[1, 8, 20] Proteomes (1 mg/mL) were pretreated with compounds at indicated concentrations (30 min, 37 °C) followed by labeling with either FP-rhodamine or HT-01 (1 μM final concentration) in a 50 μL total reaction volume. After 30 min or 1 hr at 37 °C, the FP-rhodamine- or

HT-01-labeled reactions, respectively, were quenched with SDS-PAGE loading buffer. After separation by SDS-PAGE (10% acrylamide), samples were visualized by in-gel fluorescence scanning using a flatbed fluorescent scanner (Hitachi FMBio IIe). For measurement of recombinant DAGLβ activity, proteomes were diluted to 0.3 mg/mL in assay buffer (50 mM HEPES, pH 7.2, 100 mM NaCl, 5 mM CaCl2, 0.1% v/v TX-100, 10% v/v DMSO) and subjected to ABPP analysis as described above.

Abpp-Silac

Neuro2A cells were grown for 10 passages in either light or heavy SILAC DMEM medium supplemented with 10% (v/v) dialyzed FCS and 2 mM L-glutamine. Light medium was supplemented with 100 μg/mL L-arginine and 100 μg/mL L-lysine while heavy medium was supplemented with 100 μg/mL [$^{13}C_6{}^{15}N_4$]-L-Arginine and 100 μg/mL [$^{13}C_6{}^{15}N_2$]-L-Lysine. Heavy cells (in 10 mL medium) were treated with test compound and light cells were treated with DMSO for 4 hr at 37 °C. Cells were washed with PBS (2×), harvested, and lysed by sonication in DPBS. Membrane and soluble proteomes were isolated as described above and adjusted to a final concentration of 2.0 mg/mL and labeled with 10 μM FP-biotin (500 μL total reaction volume) for 2 hr at 25 °C. After incubation, light and heavy proteomes were mixed in 1:1 ratio, and excess FP-biotin removed by $CHCl_3$/MeOH extraction. To the light and heavy mixed proteomes (1 mL volume), we added 2 mL MeOH, 0.5 mL $CHCl_3$, 1.5 mL H_2O, vortexed, and centrifuged at 1,400 × *g* for 3 min. The top (aqueous) and bottom (organic) layers were removed and 600 μL of MeOH was added to the protein interface, which was subsequently transferred to a microfuge tube. Next, 150 μL of $CHCl_3$ and 600 μL of H_2O was added, vortexed, and centrifuged as described above. The top and bottom layers were removed, the protein interface sonicated in 600 μL of MeOH, and then centrifuged at 14,000 rpm for 5 min to pellet protein. The MeOH was removed and pellet resuspended in 6 M urea/25 mM ammonium bicarbonate. Samples were then reduced with 10 mM DTT for 15 min (65 °C) and alkylated with 10 mM iodoacetamide for 30 min at 25 °C in the dark. Afterwards, samples were treated with SDS (2% final, 5 min) and biotinylated proteins enriched with avidin beads (50 μL beads; conditions: 1 hr, 25 °C, 0.5% SDS in PBS). The beads were washed three times with 1% SDS in PBS followed by three washes with PBS. The urea concentration was reduced to 2 M with 2x volume DPBS. On-bead digestions were performed for 12 hr at 37 °C with sequence-grade modified trypsin (Promega; 2 μg) in the presence of 2 mM $CaCl_2$. Peptide samples were acidified to a final concentration of 5% (v/v) formic acid and stored at -80 °C prior to analysis. LC-MS/MS analysis of ABPP-SILAC samples were performed as previously described.[8, 15, 16]

In vivo studies with compounds 9, 11, and 20

Mice were injected with compounds **9**, **11**, or **20** i.p. in 18:1:1 (v/v/v) solution of saline/ethanol/PEG40 (ethoxylated castor oil, 10 μl g^{-1}). For p.o. studies with **11**, mice were administered compound by oral gavage in PEG300 (4 μl g^{-1}). For dose-response studies, mice were treated with varying doses of compounds for 4 hr, anesthetized with isoflurane, and euthanized by cervical dislocation. Animal experiments were conducted in accordance with the guidelines of the Institutional Animal Care and Use Committee of The Scripps Research Institute.

Determination of IC_{50} values

For *in vitro* analyses, proteomes were pretreated with inhibitor for 30 min at 37 °C at the indicated concentrations ($n = 3$) followed by labeling with HT-01 or FP-rhodamine (1 μM probe) for 30 min at 37 °C. For *in situ* measurements, Neuro2A cells were treated with varying concentrations of compound ($n = 3$) in serum-free media (4 hr, 37 °C with 5% CO_2), lysed, and proteomes prepared for ABPP analysis as described above. After quenching, SDS-PAGE, and in-gel visualization, the percentage of enzyme activity remaining was determined by measuring the integrated optical intensity of the bands using ImageJ software. Nonlinear regression analysis was used to determine the IC_{50} values from a dose-response curve generated using GraphPad Prism.

Supplementary Material

Refer to Web version on PubMed Central for supplementary material.

Acknowledgments

This work was supported by the National Institutes of Health Grants DA017259 (B.F.C.) and DA033760 (B.F.C.), a Hewitt Foundation Postdoctoral Fellowship (K.L.H.), the Skaggs Institute for Chemical Biology, and Dainippon Sumitomo Pharma (K.T.)

References

1. Bachovchin DA, Ji T, Li W, Simon GM, Blankman JL, Adibekian A, Hoover H, Niessen S, Cravatt BF. Superfamily-wide portrait of serine hydrolase inhibition achieved by library-versus-library screening. Proc Natl Acad Sci U S A. 2010; 107:20941–20946. [PubMed: 21084632]
2. Long JZ, Cravatt BF. The metabolic serine hydrolases and their functions in mammalian physiology and disease. Chem Rev. 2011; 111:6022–6063. [PubMed: 21696217]
3. Blankman JL, Simon GM, Cravatt BF. A Comprehensive Profile of Brain Enzymes that Hydrolyze the Endocannabinoid 2-Arachidonoylglycerol. Chem Biol. 2007; 14:1347–1356. [PubMed: 18096503]
4. Li W, Blankman JL, Cravatt BF. A functional proteomic strategy to discover inhibitors for uncharacterized hydrolases. J Am Chem Soc. 2007; 129:9594–9595. [PubMed: 17629278]
5. Marrs WR, Blankman JL, Horne EA, Thomazeau A, Lin YH, Coy J, Bodor AL, Muccioli GG, Hu SS, Woodruff G, Fung S, Lafourcade M, Alexander JP, Long JZ, Li W, Xu C, Moller T, Mackie K, Manzoni OJ, Cravatt BF, Stella N. The serine hydrolase ABHD6 controls the accumulation and efficacy of 2-AG at cannabinoid receptors. Nat Neurosci. 2010; 13:951–957. [PubMed: 20657592]
6. Tchantchou F, Zhang Y. Selective inhibition of alpha/beta-hydrolase domain 6 attenuates neurodegeneration, alleviates blood brain barrier breakdown, and improves functional recovery in a mouse model of traumatic brain injury. J Neurotrauma. 2013; 30:565–579. [PubMed: 23151067]
7. Navia-Paldanius D, Savinainen JR, Laitinen JT. Biochemical and pharmacological characterization of human alpha/beta-hydrolase domain containing 6 (ABHD6) and 12 (ABHD12). J Lipid Res. 2012; 53:2413–2424. [PubMed: 22969151]
8. Hsu KL, Tsuboi K, Adibekian A, Pugh H, Masuda K, Cravatt BF. DAGLbeta inhibition perturbs a lipid network involved in macrophage inflammatory responses. Nat Chem Biol. 2012; 8:999–1007. [PubMed: 23103940]
9. Hsu KL, Tsuboi K, Whitby LR, Speers AE, Pugh H, Inloes J, Cravatt BF. Development and optimization of piperidyl-1,2,3-triazole ureas as selective chemical probes of endocannabinoid biosynthesis. J Med Chem. 2013 in Press.
10. Hsu, KL.; Tsuboi, K.; Speers, AE.; Brown, SJ.; Spicer, T.; Fernandez-Vega, V.; Ferguson, J.; Cravatt, BF.; Hodder, P.; Rosen, H. Probe Reports from the NIH Molecular Libraries Program [Internet]. Bethesda (MD): National Center for Biotechnology Information (US); 2012.

Optimization and characterization of triazole urea inhibitors for abhydrolase domain containing protein 6 (ABHD6). updated Mar 14 2013

11. Rostovtsev VV, Green LG, Fokin VV, Sharpless KB. A Stepwise Huisgen Cycloaddition Process: Copper(I)-Catalyzed Regioselective "Ligation" of Azides and Terminal Alkynes. Angew Chem Int Ed. 2002; 41:2596–2599.
12. Speers AE, Adam GC, Cravatt BF. Activity-Based Protein Profiling in Vivo Using a Copper(I)-Catalyzed Azide-Alkyne [3 + 2] Cycloaddition. J Am Chem Soc. 2003; 125:4686–4687. [PubMed: 12696868]
13. Nagano JM, Hsu KL, Whitby LR, Niphakis MJ, Speers AE, Brown SJ, Spicer T, Fernandez-Vega V, Ferguson J, Hodder P, Srinivasan P, Gonzalez TD, Rosen H, Bahnson BJ, Cravatt BF. Selective inhibitors and tailored activity probes for lipoprotein-associated phospholipase A(2). Bioorg Med Chem Lett. 2013; 23:839–843. [PubMed: 23260346]
14. Kalisiak J, Sharpless KB, Fokin VV. Efficient Synthesis of 2-Substituted-1,2,3-triazoles. Org Lett. 2008; 10:3171–3174. [PubMed: 18597477]
15. Adibekian A, Martin BR, Wang C, Hsu KL, Bachovchin DA, Niessen S, Hoover H, Cravatt BF. Click-generated triazole ureas as ultrapotent in vivo–active serine hydrolase inhibitors. Nat Chem Biol. 2011; 7:469–478. [PubMed: 21572424]
16. Bachovchin DA, Mohr JT, Speers AE, Wang C, Berlin JM, Spicer TP, Fernandez-Vega V, Chase P, Hodder PS, Schurer SC, Nomura DK, Rosen H, Fu GC, Cravatt BF. Academic cross-fertilization by public screening yields a remarkable class of protein phosphatase methylesterase-1 inhibitors. Proc Natl Acad Sci U S A. 2011; 108:6811–6816. [PubMed: 21398589]
17. Long JZ, Nomura DK, Cravatt BF. Characterization of monoacylglycerol lipase inhibition reveals differences in central and peripheral endocannabinoid metabolism. Chem Biol. 2009; 16:744–753. [PubMed: 19635411]
18. Liu Y, Patricelli MP, Cravatt BF. Activity-based protein profiling: the serine hydrolases. Proc Natl Acad Sci U S A. 1999; 96:14694–14699. [PubMed: 10611275]
19. Kidd D, Liu Y, Cravatt BF. Profiling serine hydrolase activities in complex proteomes. Biochemistry. 2001; 40:4005–4015. [PubMed: 11300781]
20. Jessani N, Niessen S, Wei BQ, Nicolau M, Humphrey M, Ji Y, Han W, Noh DY, Yates JR 3rd, Jeffrey SS, Cravatt BF. A streamlined platform for high-content functional proteomics of primary human specimens. Nat Methods. 2005; 2:691–697. [PubMed: 16118640]

Abbreviations Used

ABPP	activity-based protein profiling
SH	serine hydrolase
2-AG	2-arachidonoylglycerol
Pip-1,2,3-TU	piperidyl-1,2,3-triazole urea
CuAAC	copper-catalyzed azide alkyne cycloaddition
FP-Rh	fluorophosphonate-rhodamine
SILAC	stable isotope labeling by amino acids in cell culture

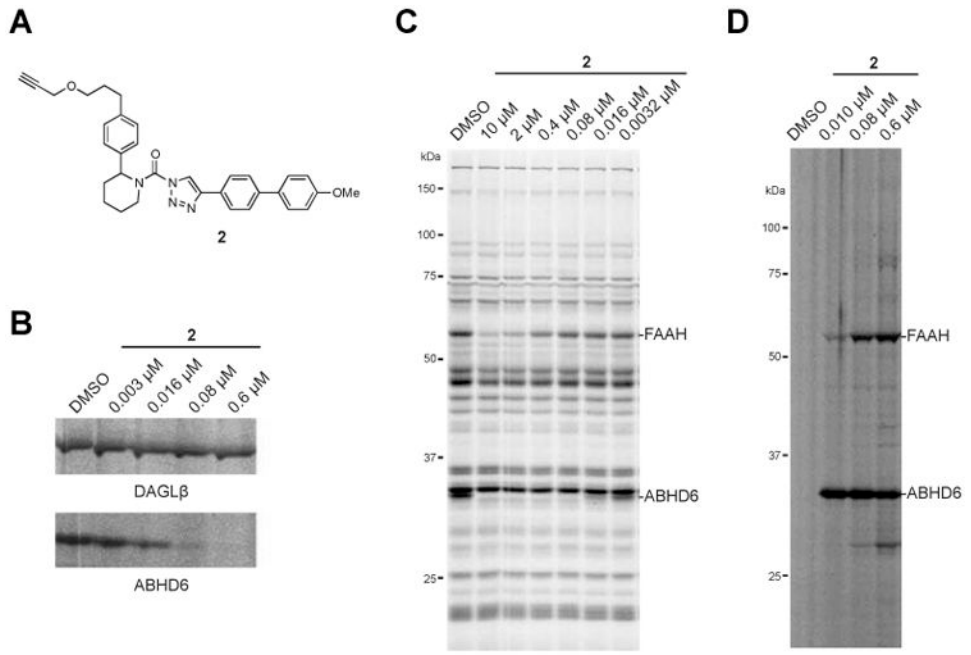

Figure 1.

Structure and activity of compound **2**, a clickable analogue of **1**. (A) Chemical structure of compound **2**. (B) *In vitro* potency of compound **2** against DAGLβ and ABHD6 in Neuro2A membrane proteome as measured by gel-based competitive ABPP using the tailored activity-based probe HT-01. Neuro2A proteome (1 mg/mL) was incubated with the indicated concentrations of **2** (30 min, 37 °C) followed by labeling with 1 μM HT-01 (30 min, 37 °C), and DAGLβ and ABHD6 activity visualized by SDS-PAGE and in-gel fluorescence scanning. (C) Selectivity of compound **2** against mouse brain membrane SH enzymes as measured by gel-based competitive ABPP using the broad-spectrum, SH-directed probe FP-Rh. (D) Click chemistry-ABPP of Neuro2A cells treated *in situ* with compound **2**. Neuro2A cells were treated with the indicated concentrations of compound **2** (1 hr, 37 °C), lysed, and compound **2**-labeled proteins visualized in the membrane proteome by click chemistry reaction with azide-Rh followed by SDS-PAGE and in-gel fluorescence scanning. Fluorescent gels are shown in gray scale. Assignment of serine hydrolase enzyme activities in competitive ABPP gels are based on gel migration patterns consistent with past studies.[8, 9, 13]

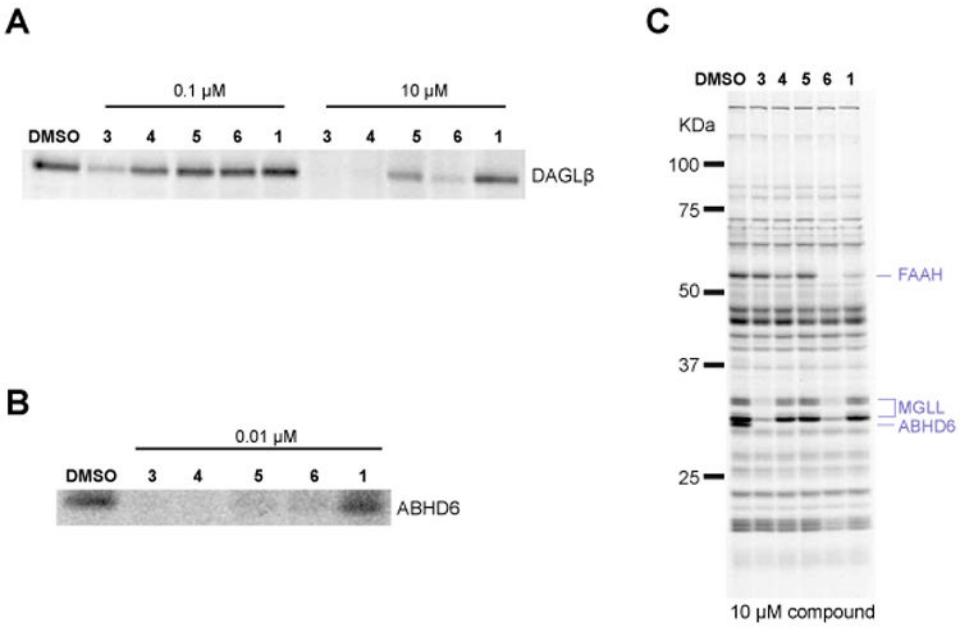

Figure 2.

Potency and selectivity of lead ABHD6 inhibitors. Potency of (2-substituted)-Pip-1,2,3-TUs against (A) recombinant DAGLβ expressed by transient transfect in HEK293T cells (DAGLβ-HEK293T lysates), and (B) endogenous ABHD6 in Neuro2A membrane proteomes as measured by gel-based competitive ABPP using the HT-01 probe. (C) Selectivity of inhibitors against mouse brain membrane SH enzymes as measured by gel-based competitive ABPP using the FP-Rh probe. For the gel-based ABPP assays, proteomes were incubated with compound (0.01, 0.1 or 10 μM) for 30 min at 37 °C followed by reaction with fluorescent ABPP probes (HT-01 or FP-Rh, 1 μM, 30 min, 37 °C). Fluorescent gel images are shown in gray scale. Serine hydrolase activities in gels were assigned as described in Figure 1.

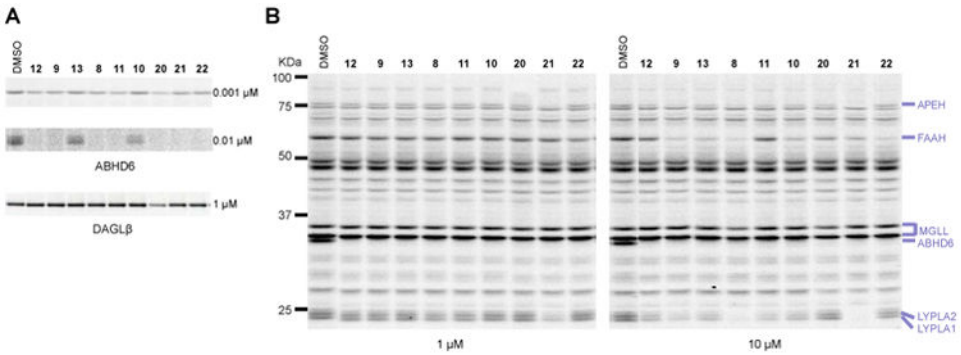

Figure 3.

Potency and selectivity of advanced ABHD6 inhibitors. (A) Potency of (2-substituted)-Pip-1,2,3-TUs against ABHD6 in Neuro2A cell membranes or DAGLβ-HEK293T lysates by gel-based competitive ABPP using the HT-01 probe. (B) Selectivity of (2-substituted)-Pip-1,2,3-TUs against mouse brain SHs as measure by gel-based competitive ABPP using the FP-Rh probe. Gel-based ABPP assays were performed as described in Figure 1. Fluorescent gel images are shown in gray scale. Serine hydrolase activities in gels were assigned as described in Figure 1.

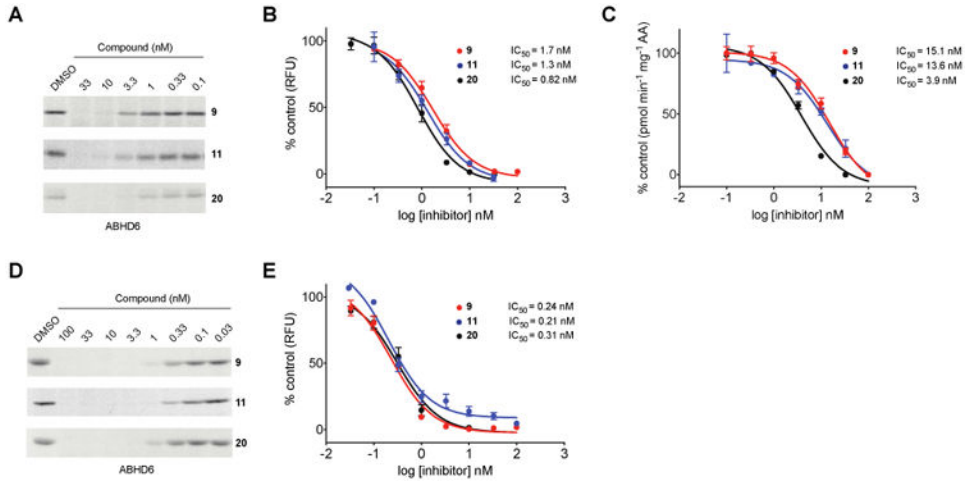

Figure 4.

In vitro (A-C) and *in situ* (D, E) IC_{50} values for compounds **9**, **11**, and **20** against ABHD6 as determined by gel-based competitive ABPP with the activity-based probe, HT-01 (A, B, D, E) and 2-AG substrate hydrolysis assays (C). For *in vitro* gel-based ABPP studies (A, B), Neuro2A membrane proteomes were preincubated with varying concentrations of compounds for 30 min at 37 °C, treated with HT-01 (1 μM, 30 min, 37 °C), quenched in SDS-PAGE loading buffer, and analyzed by in-gel fluorescence scanning. For 2-AG hydrolysis assays (C), inhibitors were tested against ABHD6 recombinantly expressed in HEK293T cells as described in the **Experimental Section**. For *in situ* studies (D, E), Neuro2A cells were treated with varying amounts of compounds for 4 hr, lysed, and subjected to competitive ABPP as described above. Integrated band intensities of probe-labeled proteins were calculated using ImageJ and used to generate concentration-dependent inhibition curves for both *in vitro* (B) and *in situ* (E) studies.

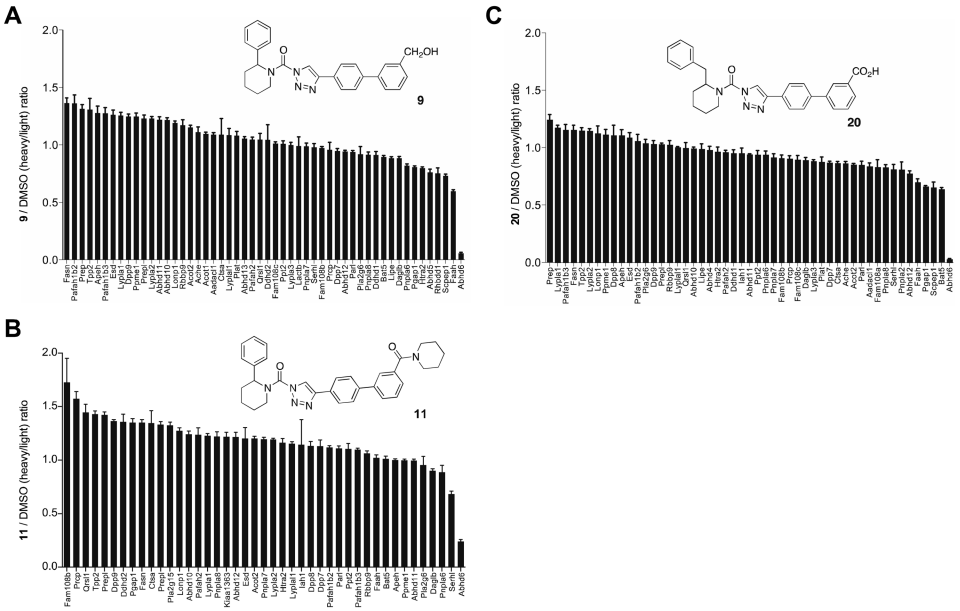

Figure 5.

In situ activity and selectivity of ABHD6 inhibitors in Neuro2A cells. ABPP-SILAC analysis of SH activities from Neuro2A cells treated *in situ* with 3 nM of compound **9** (A), **11** (B), or **20** (C) for 4 hr. Error bars represent mean ± s.e.m. of heavy/light ratios for the multiple quantified peptides observed for each enzyme (minimum of 3 unique peptides per enzyme) in both soluble and membrane fractions.

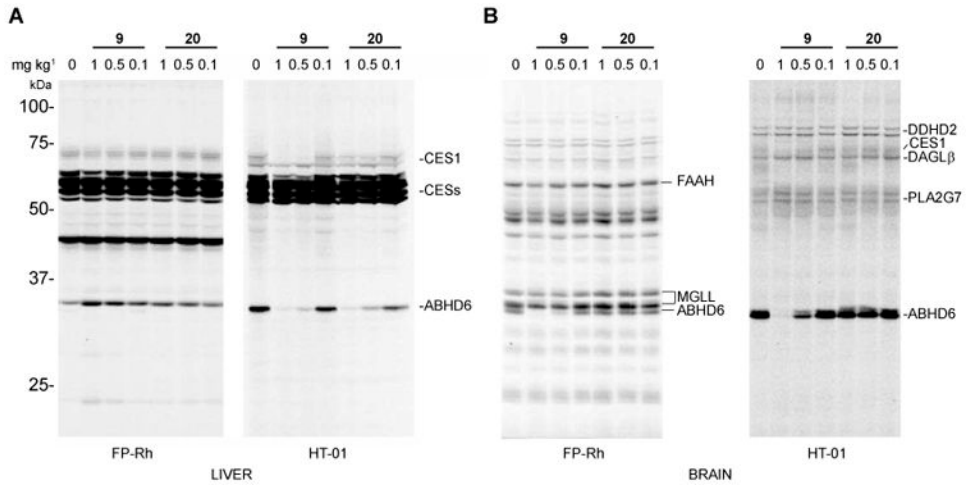

Figure 6.

Comparative analysis of the potency and selectivity of compounds **9** and **20** *in vivo* in mouse liver (A) and brain (B). Mice were administered vehicle or test compounds (1, 0.5, or 0.1 mg kg^{-1}, i.p.), and, after 4 hr, sacrificed and their brain and liver tissues harvested, the membrane fractions isolated, and subjected to gel-based competitive ABPP with FP-Rh or HT-01 (1 μM, 30 min, 37 °C). Compound **9** produced near-complete inactivation of ABHD6 at 1 mg kg^{-1} in both liver (A, HT-01 gel) and brain (B, FP-Rh or HT-01 gels), while **20** showed peripherally restricted activity with near-complete inactivation of ABHD6 in liver, but not brain at at 1 mg kg^{-1}. For gel-based ABPP experiments, proteomes were labeled with FP-Rh or HT-01 (1 μM probe) for 30 min at 37 °C. Note that ABHD6 was too low in abundance in liver for robust detection by the FP-Rh probe under the described assay conditions. Serine hydrolase activities in gels were assigned as described in Figure 1.

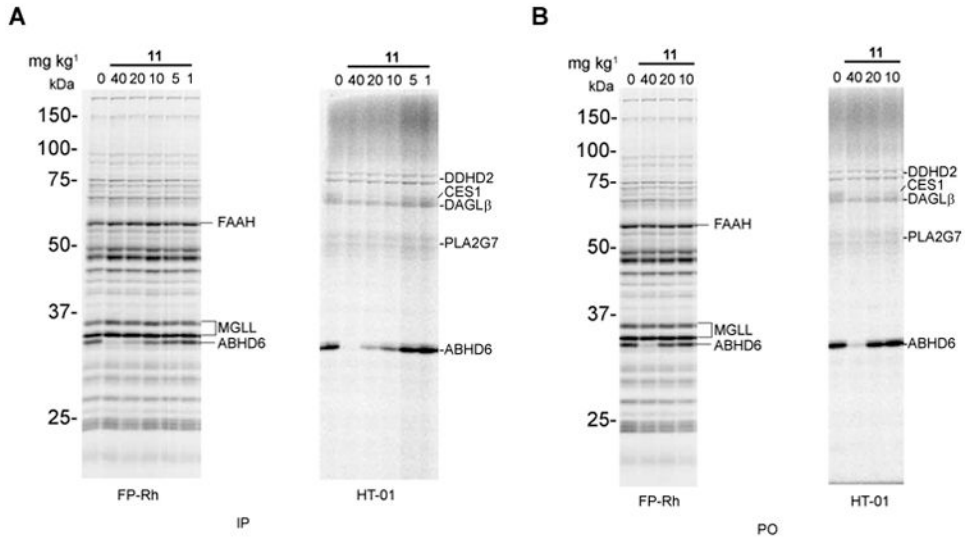

Figure 7.

Potency and selectivity of compound **11** in the mouse brain *in vivo*. (A) Mice were administered vehicle or compound **11** (1-40 mg kg^{-1}, i.p.), and, after 4 hr, sacrificed and brain tissue harvested, the membrane fractions subjected to gel-based competitive ABPP with FP-Rh or HT-01 (1 μM, 30 min, 37 °C). Compound **11** completely inactivated ABHD6 at 40 mg kg^{-1} with partial blockade at lower doses (>70 % inhibition at 20 mg kg^{-1}) and showed excellent selectivity against other brain SHs, including negligible cross-reactivity with FAAH across the entire tested dose-range. (B) Compound **11** administered to mice by oral gavage (p.o.) produced near-complete and selective inactivation of brain ABHD6 at a dose of 40 mg kg^{-1}. For gel-based ABPP experiments, proteomes were labeled with FP-Rh or HT-01 (1 μM probe) for 30 min at 37 °C. Serine hydrolase activities in gels were assigned as described in Figure 1.

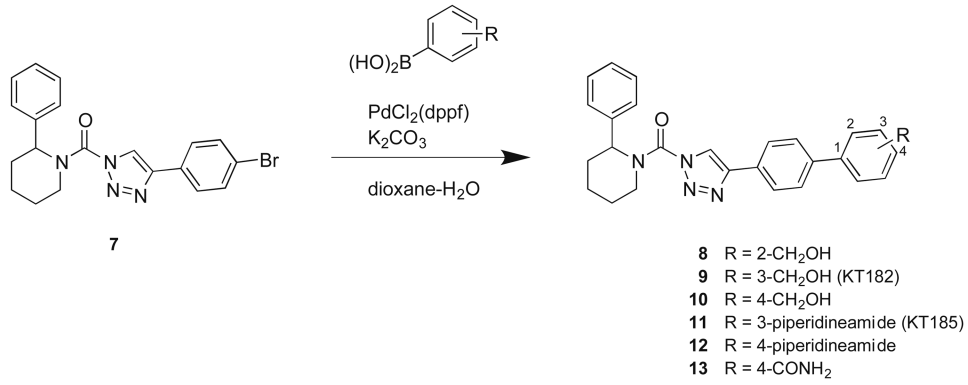

Scheme 1. Synthesis of (2-phenyl)-piperidine-1,2,3-TUs

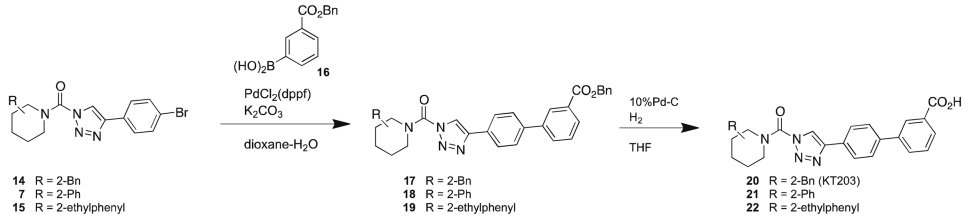

Scheme 2. Synthesis of carboxylate-modified (2-substituted)-Pip-1,2,3-TU ABHD6 inhibitors

Table 1

Structure-activity relationship of lead ABHD6 inhibitors.

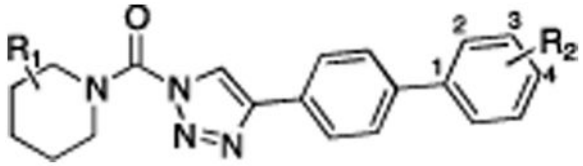

Compound	R_1=	R_2 =	DAGLβ % Inhibition (100 nM)	DAGLβ % Inhibition (10 μM)	ABHD6 % Inhibition (10 nM)	Off-targets (10 μM)
1 (KT195)	2-Ph	4-OMe	0	0	30	FAAH
3	2-Bn	2-OMe	66	100	89	MGLL
4	2-Bn	3-CH_2OH	37	91	91	none
5	2-Bn	4-piperidineamide	15	58	79	none
6	2-Ph	2-OMe	14	70	82	FAAH, MGLL

Table 2

Activity of (2-phenyl)-piperidine-1,2,3-TUs

Compound	ABHD6 % Inhibition (10 nM)	ABHD6 % Inhibition (1 nM)	DAGLβ Inhibition (1 μM)	Off-targets (1 μM)	Off-targets (10 μM)
8	98	38	0	none	FAAH, LYPLA1, LYPLA2
9	84	29	0	none	FAAH, LYPLA1, LYPLA2
10	47	18	0	none	FAAH, LYPLA1, LYPLA2
11	100	51	0	none	LYPLA1, LYPLA2
12	94	35	0	none	LYPLA1, LYPLA2
13	27	17	0	none	FAAH, LYPLA1, LYPLA2
20	100	62	50	none	FAAH, DAGLβ
21	100	36	6	APEH, LYPLA1, LYPLA2	FAAH, APEH, LYPLA1, LYPLA2
22	94	33	4	none	FAAH

J Med Chem. Author manuscript; available in PMC 2014 November 14.